Title
Inhibition of Soluble Epoxide Hydrolase Reduces Paraquat Neurotoxicity in Rodents

Author
Atone, Jogen

Publication Date
2022

Peer reviewed|Thesis/dissertation

Inhibition of Soluble Epoxide Hydrolase Reduces Paraquat Neurotoxicity in Rodents

By

JOGEN ATONE

THESIS

Submitted in partial satisfaction of the requirements for the degree of

MASTER OF SCIENCE

in

Pharmacology and Toxicology

in the

OFFICE OF GRADUATE STUDIES

of the

UNIVERSITY OF CALIFORNIA

DAVIS

Approved:

Bruce D. Hammock, Chair

Heike Wulff

Pamela Lein

Committee in Charge

2022

Acknowledgments

Firstly, I would like to acknowledge my PI, Dr. Bruce Hammock, for facilitating my growth as a scientist by allowing me the freedom to explore and learn from many of the talented researchers in the laboratory. He has shared with me countless valuable insights necessary to become a productive scientist and has motivated me throughout my time in this lab, and I cannot thank him enough for allowing me this opportunity for growth. In addition to Dr. Hammock, I would like to acknowledge everybody in the laboratory including Christophe Morisseau, Sung Hee Hwang, Cindy McReynolds, and particularly Karen Wagner and Naoki Matsumoto for detailed instructions on rodent handling and cell culture work, respectively. I could not have achieved any significant feat without all the generous help offered by everybody in my lab.

Secondly, I would like to thank Dr. Heike Wulff and Dr. Hai Minh Nguyen for continuous support in the primary cell culture work, for guidance on immunostaining, and for offering me countless pieces of advice throughout my graduate school career. In addition, Dr. Aldrin Gomes and Dr. Koike Shinichiro from Dr. Fawaz Haj lab have offered me insights and detailed instructions to perform the delicate task of western blotting, and Dr. Pamela Lein and her lab team for instructions and training on primary cell harvesting as well as valuable critiques. I would like to express my deepest gratitude to everyone who has supported me, including those not mentioned here explicitly.

Abstract

Paraquat is one of the most common and acutely toxic herbicides used in developing nations, with epidemiological studies linking chronic paraquat exposure to Parkinson's disease. Numerous studies in mice have demonstrated a chronic paraquat-mediated reduction in dopaminergic neural markers in the midbrain. However, given the scarcity of research surrounding the effect of chronic paraquat on striatal neurotoxicity, there is a need for further investigation into the effect of paraquat on the induction of endoplasmic reticulum stress and inflammation in mouse striatum. This study attempts to observe changes in both inflammatory and endoplasmic reticulum stress markers in mouse striatum following chronic paraquat administration. Furthermore, previous studies have shown that inhibition of soluble epoxide hydrolase mitigates MPTP-mediated loss of dopaminergic neurons and endoplasmic reticulum stress in mouse striatum. Thus, this study seeks to determine if inhibition of soluble epoxide hydrolase mitigates paraquat-induced neurotoxicity, as well as whether epoxyeicosatrienoic acids, endogenous substrates of the soluble epoxide hydrolase, reduce TLR4-mediated inflammation in primary astrocytes and microglia. Our results show that while the pro-inflammatory effect of chronic paraquat injection on mouse striata is relatively small, there are significant inductions of inflammatory and cellular stress markers such as COX2 and CHOP *in vivo* and inflammatory markers *in vitro* that can be mitigated through a prophylactic administration of a soluble epoxide hydrolase inhibitor.

Inhibition of Soluble Epoxide Hydrolase Reduces Paraquat Neurotoxicity in Rodents

Jogen Atone[a], Karen Wagner[a], Shinichiro Koike[b], Jun Yang[a], Sung Hee Hwang[a], Bruce D. Hammock*[a]

[a]Department of Entomology and Nematology, and UC Davis Comprehensive Cancer Center, University of California Davis, Davis, CA 95616

[b]Department of Nutrition, University of California Davis, Davis, CA 95616

*Corresponding author. Tel.: +1-530-752-7519

E-mail address: bdhammock@ucdavis.edu

1. Introduction

Paraquat (1,1'-dimethyl-4,4'-bipyridinium; PQ) is a non-selective contact herbicide used to control weeds and grasses around vegetables, grain, soybeans, coffee, cotton, and sugarcane among other crops (Bromilow, 2004). Following a ban on its use in the US, restricted use in the US is currently allowed after the development of new formulations and safety practices to reduce incidences of acute toxicity and fatalities (Mandel et al., 2012). Due to its effectiveness and low cost, there has been a notable recent rise in PQ use within the US in the past decade according to an estimate by U.S. Geological Survey, reaching over 15 million pounds annually by 2018 estimate (USGS, 2021). PQ has low dermal toxicity; however, its use is associated with numerous deaths following suicide attempts and/or accidental ingestion (Seok et al., 2009; Srikrishna et al., 1992). In addition to being one of the most acutely toxic pesticides worldwide (Dawson et al., 2010), PQ use has long been hypothesized to increase the risk of development of Parkinson's disease (PD) (Dinis-Oliveira et al., 2006; Tangamornsuksan et al., 2019). This is especially the case when PQ is combined with pesticides like the fungicide maneb (Bastias-Candia et al., 2019; Mandel et al., 2012), which is often a preferred experimental model given the inconsistency of toxic effects caused by PQ when administered by itself (Breckenridge et al., 2013; Jackson-Lewis et al., 2012; Thiruchelvam et al., 2000).

PQ is thought to exert its toxic effects through redox cycling with various metabolic enzymes or oxygen molecules, generating reactive oxygen species (ROS), which in turn cause apoptosis, endoplasmic reticulum (ER) stress, and inflammatory responses further exacerbating tissue damage (See et al., 2022; Wu et al., 2005). Although the risk

of dermal toxicity with PQ is very low, following systemic injection in mice, PQ accumulates in vital organs including the lung, kidney, liver, and brain, with a long tissue half-life such that significant accumulation can occur in the brain (Breckenridge et al., 2013; Campbell et al., 2021). In mice, the half-life of PQ in the brain was approximately 3 weeks (Breckenridge et al., 2013), suggesting that chronic exposure to PQ may have a serious repercussion for those who work closely with PQ. Such an ability for PQ to accumulate in mammalian tissues underscores the concern for chronic PQ exposure and subsequent toxic effects on the human population and the need for a therapeutic agent that can minimize the effect of PQ exposure (Fig. 1). Given that inflammation and ER stress often follows exposure to environmental neurotoxicants and accompany neurodegenerative disorders such as PD (McGeer and McGeer, 2004; Yang et al., 2020; Yoshida, 2007), a therapeutic agent that mitigates both effects of neurotoxicity may be ideal. Inhibitors of soluble epoxide hydrolase (sEH), which metabolizes epoxy-fatty acids (EpFA) into their corresponding diols (Morisseau et al., 2010) are known to shift ER stress from initiation of inflammation, pain, and cell senescence toward cellular homeostasis and resolution of inflammation and pain (Atone et al., 2020; Wagner et al., 2017). Thus, sEH inhibitors may be useful tools to reduce PQ-induced ER stress and inflammation, given that their mechanism involves reduction of inflammation, ER stress, apoptosis, and ROS among other benefits (Atone et al., 2020).

Past research has studied sEH inhibitors as potential therapeutic candidates in numerous animal models of neuropathology, including stroke, traumatic brain injury, and more recently 1-methyl-4-phenyl-1,2,3,6-tetrahydropyridine (MPTP)-induced

neurotoxicity (Hung et al., 2017; Qin et al., 2015; Ren et al., 2018; Simpkins et al., 2009). While the precise mechanism of action of the EpFA is still under investigation, sEH inhibitors are known to increase the concentrations of endogenous EpFA, such as the epoxyeicosatrienoic acids (EETs) derived from arachidonic acid. Like other classes of EpFA, EETs have been demonstrated to have anti-inflammatory and anti-apoptotic effects in numerous animal and cellular models (Hung et al., 2017; Tu et al., 2018).

Several studies have demonstrated a neuroprotective role of sEH inhibitors against the dopaminergic neurotoxicants MPTP and rotenone, evident as mitigation of inflammation, ER stress, and loss of tyrosine hydroxylase (TH)-immunopositive neurons (Lakkappa et al., 2019; Ren et al., 2018). PQ toxicity has been characterized by the induction of ER stress and inflammation in cellular models of PQ neurotoxicity (Li et al., 2015a; See et al., 2022; Yang et al., 2020). In addition, PQ is known to induce inflammation and ER stress in several organs of mice, most notably in the heart and lungs (Lei et al., 2017). Given the broad systemic distribution of PQ and its accumulation in mouse midbrain (Breckenridge et al., 2013), we hypothesized that inflammatory and ER stress markers would be elevated in the striatum following a 3-week administration of PQ. Further, we hypothesized that sEH inhibition would mitigate these endpoints of PQ-induced neurotoxicity.

In addition, many pesticides and pollutants induce neuroinflammation via a toll-like receptor 4 (TLR4) dependent pathway including PQ, organophosphate pesticides, dioxins, and ionizing radiation (Lucas and Maes, 2013; Yang et al., 2022). PQ does not cause direct glial activation in mice but rather induces neuroinflammation through

dopamine neural damage, inducing a TLR4 mediated activation (Klintworth et al., 2009; Wu et al., 2005; Yang et al., 2022). Here, we have assessed the effect of TPPU and EETs on primary astrocytes and microglia activated by a TLR4 ligand LPS. Since it was previously shown that TPPU may be effective against LPS-induced glial inflammation in mice (Ghosh et al., 2020), in this study we tested our hypothesis on rat glial cells with EETs regioisomers to expand our understanding of the scope of their therapeutic potential.

2. Methods

2.1 Animal Treatment

In-life procedures and husbandry performed at the University of California, Davis adhered to the guidelines of the National Institutes of Health Guide for the Care and Use of Laboratory Animals and were performed in accordance with the protocols approved by the Animal Use and Care Committee (IACUC) of the University of California, Davis. Male C57BL/6J mice (8-10 weeks; 20-25 g) were obtained from The Jackson Laboratory and were acclimated in our vivarium under a 12 h light/dark cycle for one week prior to pre-treatment with the sEH inhibitor 1-trifluoromethoxyphenyl-3-(1-propionylpiperidin-4-yl) urea (TPPU; 12 mg/L in 1% PEG-400 drinking water) or vehicle (1% PEG-400 in drinking water) control. TPPU was synthesized in-house as previously described (Rose et al., 2010). The dose of TPPU was calculated based on the observed volume of water consumption to yield approximately 2 mg/kg/day. Tail vein blood was sampled to quantify the TPPU concentration via LC-MS/MS to verify sufficient systemic exposure at the conclusion of the experiment (Fig. S1). The mice were assessed throughout the experiment for weight and water consumption (Fig. S2).

Formulated drinking water and chow were provided ad libitum. One week after the initiation of the treated drinking water, the mice were injected with either PQ (10 mg/kg, *i.p.*; purity: 98%; ThermoFisher; Cat. 227320050, Lot: A0397584) or vehicle (sterile phosphate-buffered saline; PBS; ThermoFisher). PQ solutions were dissolved in sterile PBS, stored in -80°C until use, and were injected into mice twice weekly for 3 weeks for a total of 6 injections. This dosage regime has been previously used for inducing chronic PQ neurotoxicity, with pharmacokinetic data verifying a chronic accumulation of PQ in a mouse midbrain (Gupta et al., 2010; Prasad et al., 2009). Five days after the final PQ injection, the mice were euthanized via cervical dislocation upon inhalation of isoflurane anesthetic. Striatum samples between +1 mm and bregma were obtained on ice, washed in PBS, and flash frozen in liquid nitrogen for Western blot and RT-qPCR analysis. Alternatively, striatum samples were fixed in a 4% paraformaldehyde (PFA) solution in Phosphate-based saline (PBS; Apex Bioresearch Products; Cat. 20-134) for 48 hours, after which the samples were paraffinized and sectioned for immunohistochemical (IHC) analyses. Samples were obtained immediately after euthanasia without perfusion and thus contain small amounts of blood. The MPTP group received five intraperitoneal injections of MPTP (30 mg/kg/day; purity: >98%; MedChemExpress; Cat. HY-100852) dissolved in PBS once a day while the control group received sterile PBS (100 µL/day; *i.p.*) for five days. Mice were euthanized with isoflurane and cervical dislocation 1 week following the final injection and their striata were either flash frozen for RT-qPCR or fixed in 4% PFA solution in PBS for subsequent paraffin embedding and IHC analysis.

2.2 Primary glial cell isolation and cell culture

Primary glial cells (>90% astrocytes) were isolated from the cortex of postnatal day 1-2 (P1-2) Sprague-Dawley rats (Charles River Laboratories). P1-2 rat pups were decapitated, their cortex isolated, dura and meninges removed, tissues mechanically homogenized with a sterile razor and triturated with a sterile fire-polished Pasteur pipette, and the cells were strained using a 40 μm cell strainer (Spectrum Chemical). Resulting cells were plated onto a T75 plate coated with poly-L-lysine (MilliporeSigma; molecular weight 150,000-300,000) at a density of 6.0 x 10^5 cells per cm^2 and cultured in DMEM (Corning) with 10% fetal bovine serum (FBS; ThermoFisher) for 8 days. On DIV 9, glial cells were plated onto a poly-L-lysine coated 96 well plate at a density of 6.25 X 10^5 cells per cm^2 and cultured overnight for experimentation the next day. The mixture consists of astrocytes and microglia, with approximately 90% GFAP+ astrocytes and 10% IBA+ microglia when assessed via immunocytochemistry (data not shown).

2.3 RT-qPCR

To assess the efficacy of the sEH substrates on glial cell activation, 1 μM each of EETs (14,15-EET, 11,12-EET, 8,9-EET, or a 1:1:1 mixture ratio), all ±1 μM TPPU in 10% FBS DMEM with 0.1% sterile DMSO were applied to primary rat glial cells (DIV 10). EETs were synthesized and purified as recently discussed by Singh et al. (Singh et al., 2021). Purity was assessed via thin layer chromatography and nuclear magnetic resonance (data not shown). 5,6-EET was not included due to its unique susceptibility to nonenzymatic or cyclooxygenase mediated cyclization (Carroll et al., 1993) and nonenzymatic conversion to the corresponding diol (DHET) (Jiang et al., 2004). The solutions of EETs and EETs mixtures and TPPU were prepared by adding them in

DMSO and diluted in DMEM to give a final concentration of 1 μM, a level previously shown to reduce LPS-induced nitrite release in primary glial cells (Ghosh et al., 2020), with less than 0.1% DMSO at the final concentration in media. LPS from *Salmonella typhosa* (potency: >500000 EU/mg; MilliporeSigma; Cat. L2387, Lot:117M4057V) dissolved in DMEM was then added to each well and the cells were incubated at 37 °C for 24 h at a final concentration of 300 ng/ml. RNA was extracted using a TRIzol reagent according to the manufacturer's protocol. Alternatively, frozen striata collected from mice were pulverized and RNA was extracted similarly using a TRIzol reagent. The RNA concentration and 260/280 values were assessed using NanoDrop Lite Spectrophotometer (ThermoFisher, Waltham, MA). For each reaction, 6 μL RNA (100 ng) was mixed with 9 μL Luna Universal One-Step RT-qPCR Kit Master Mix (Cat. E3005L, New England Biolabs) containing 8 μM of primers. The fluorescence was detected using Mic qPCR Cycler (Bio Molecular Systems, El Cajon, CA). Gene expression was calculated using the Ct values obtained within the Mic qPCR Analysis software which uses the LinRedPCR method developed by Ramakers et al. (Ramakers et al., 2003). PCR product specificity was evaluated by melting curve analysis, with each product showing a single peak (data not shown). Primer sequences for RT-qPCR are listed in Table 1.

2.4 Western Blot

Mechanically pulverized frozen striatum samples were homogenized in radioimmunoprecipitation assay (RIPA) buffer (Neta Scientific) containing 1:100 protease inhibitor cocktail (MilliporeSigma), centrifuged for 30 minutes at 12,000 g at 4°C, and protein concentrations were assessed using a BCA assay (ThermoFisher). SDS-

PAGE was performed on 10% SDS tris-glycine gels using 20 μg protein per lane (BioRad). The membranes were blocked using EveryBlot Blocking Buffer (BioRad) for 5 minutes, followed by primary antibody incubation overnight at 4°C in EveryBlot at 1:1000 concentration using the following antibodies: mouse anti-NFκB (Cell Signaling Cat. 8242S, Lot: 16), rabbit anti-ATF4 (Cell Signaling Cat. 11815S, Lot: 4), rabbit anti-eIF2α (Cell Signaling Cat. 5324S, Lot: 6), mouse anti-CHOP (Cell Signaling Cat. 2895S, Lot: 13), mouse anti-4-HNE (R&D Systems Cat. MAB3249, Lot: WXN0521121), and mouse anti-β-actin (MilliporeSigma Cat. A5316, Lot: D0615). Membranes were incubated in anti-mouse or anti-rabbit horse radish peroxidase (HRP)-conjugated secondary antibodies (Cell Signaling) at 1:5000 in 0.1% TBS-T for 1 hour at room temperature. Enhanced chemiluminescence was performed using ProSignal Pico detection reagent (Genesee Scientific).

2.5 Immunohistochemistry

Striatum sections obtained from mice were fixed in a 4% paraformaldehyde in PBS for 48 hours followed by 70% ethanol solution for a week prior to paraffinization. Paraffin sections (5 μM sections) were prepared by the Histology Core within UC Davis Department of Pathology and Laboratory Medicine. Sections were dewaxed in xylene and rehydrated using an ethanol gradient of 100%, 95%, 70%, 50%, 30%, and 0% ethanol in distilled water. Antigenic determinants were retrieved by microwaving the sections on high for 15 minutes in 10 mM Na citrate (pH 6.0) solution. Endogenous peroxidases were inactivated by immersing sections in a 1% H_2O_2 solution for 15 minutes. Sections were blocked with 5% goat serum in PBS for 1 hour and stained overnight at 4 °C with 1:4000 tyrosine hydroxylase (TH) antibody (Cell Signaling, Cat. 2792, Lot: 6) in PBS with 2% goat

plasma. Sections were then incubated with anti-rabbit biotinylated secondary antibody (Cell Signaling, Cat. 14708, Lot: 2) for 1 hour at room temperature in PBS with 2% goat plasma, and signal was amplified using VECTASTAIN Elite ABC-HRP Kit (Vector Laboratories). The tissue was visualized using 3,3'-diaminobenzidine (DAB Substrate Kit for Peroxidase, Vector Laboratories), and sections were mounted using Cytoseal 60 (ThermoFisher). Slides were imaged at 4x magnification and analyzed using ImageJ image analysis software (ver.1.52).

2.6 Blood and plasma extraction and LC/MS analysis

Blood samples (10 μL) were collected from mice tail veins of control and TPPU-treated mice in an Eppendorf tube containing EDTA to yield a final EDTA concentration of 2 mg/ml 1 day prior to behavioral testing and euthanasia TPPU was extracted using liquid-liquid extraction with 200 μL ethyl acetate, dried using a speed vacuum concentrator, and reconstituted in a 50 μL of 100 nM CUDA methanol solution. LC-MS/MS was conducted according to previously published methods (Wan et al., 2019). The liquid chromatography system used for analysis was an Agilent 1200 SL liquid chromatography series (Agilent Corporation, Palo Alto, CA). Liquid chromatography was performed on a PursuitPlus C18 2.0×150 mm, 5μm column (Varian Inc. Palo Alto, CA). Mobile phase A was water containing 0.1% glacial acetic acid, and mobile phase B consisted of acetonitrile with 0.1% glacial acetic acid. Gradient elution was performed at a flow rate of 250 μL/min. Eluted samples were analyzed using a 4000 QTrap tandem mass spectrometer (Applied Biosystems Instrument Corporation, Foster City, CA) equipped with an electrospray source (Turbo V). The instrument was operated in positive MRM mode. Similarly, mouse plasma was collected from cardiac puncture and centrifuged in an Eppendorf tube

containing EDTA to yield a final EDTA concentration of 2 mg/ml. EET and DHET were extracted and analyzed measured using a previously published method (Yang et al., 2009). The instruments used were 6500 QTRAP+ (Sciex, Redwood City, CA) with Agilent 1260 UPLC system.

2.7 Statistical Analysis

All statistical analysis was carried out in Prism 9 analysis and graphing software (GraphPad ver. 9.3.1, San Diego, CA). One-way ANOVA with Dunnett's multiple comparisons post-hoc test was used if variables satisfied Gaussian distributions tested by Bartlett's test, and Kruskal-Wallis test with Dunnett's multiple comparisons test was used if not. Results that were $p < 0.05$ were considered significant.

3. Results

3.1 PQ-mediated changes in inflammation and ER stress

Mice were pre-treated with the sEHI TPPU in drinking water for one week, followed by a continuous TPPU treatment along with PQ injections twice weekly for three weeks. TPPU treatment in drinking water resulted in peripheral blood concentration of TPPU above 1 μM, which is orders of magnitude above the IC_{50} of 6 nM and K_i of 600 pM, and an increased 14,15-EET to 14,15-DHET ratio in plasma (Fig. S1). There were no significant differences in the amount of water consumed or the weight of mice in the PQ group (Fig. S2) for the duration of the study. Chronic PQ administration significantly increased COX2 mRNA in striatal tissues ($p<0.05$; one-way ANOVA with Dunnett's multiple comparisons test), which was not significantly reduced by TPPU (Fig. 2).

Western blots for inflammatory markers NF-κB and 4-HNE in addition to three ER stress markers ATF4, eIF2α, and CHOP showed that chronic PQ treatment significantly increased the chronic ER stress marker CHOP in the striata ($p=0.019$; one-way ANOVA with Dunnett's post-hoc, multiple comparisons), which was reduced by TPPU ($p=0.008$) (Fig. 3). PQ did not result in a striatal TH loss of a similar magnitude as MPTP treatment, though MPTP did not result in a higher inflammatory mRNA expression compared to PQ at 1 week after the final MPTP injection (Fig. S3).

3.2 Reduction of TLR4 mediated inflammatory response by TPPU and EETs

Primary rat astrocytes and microglia mixture were pre-treated with TPPU and/or EETs regioisomers for 1 hour followed by 24 hours of LPS treatment, after which GAPDH normalized mRNA expressions of inflammatory markers IL-1β, IL-6, COX2, NOS2, CXCL1, and CXCL10 were assessed. While each of the EET regioisomers alone showed equivocal efficacy, when co-administered with TPPU, each EET regioisomer similarly reduced LPS-induced inflammation in glial cells. Combined 1:1:1 EET regioisomer with TPPU treatment significantly reduced LPS-induced IL-1β, IL-6, COX2, CXCL1, and CXCL10 mRNA expression (Fig. 4). TPPU was particularly effective at improving the anti-inflammatory effects of 14,15-EET, significantly impacting the effect of 14,15-EET on IL-1β, COX2, CXCL1, and CXCL10 mRNA (Fig. 4).

4. Discussion and Conclusions

Our results indicate that chronic PQ administration significantly increased COX2 mRNA expression in the striata of mice 5 days after the final PQ injection, which was not significantly reduced by sEHI treatment. Given the peripheral blood concentration of

TPPU, this lack of effect is likely not due to dosing, absorption, or distribution of TPPU due to its exceptionally high potency as an inhibitor, high target occupancy, and slow off rate from the target enzyme (Rose et al., 2010). There was a small, but significant increase, in the expression of the ER stress protein CHOP, which was significantly reduced by TPPU. While we observed a surprising reduction of the mRNA expression of TNF-α due to PQ, which was not observed in the TPPU-treated PQ-intoxicated animals, the effects were not statistically significant. Given the large biological variability, slight changes in IL-1β, IL-6 mRNA, TNFα mRNA, and 4-HNE were statistically non-significant. In addition, we observed a substantial TH loss in the mice striata 1 week after the final MPTP injection, whereas chronic PQ treatment showed no evidence of TH loss. The lack of effect of PQ on striatal TH level was also observed in several other studies despite evidence of PQ accumulation in the midbrain (Breckenridge et al., 2013; Smeyne et al., 2016), contrary to other studies that demonstrated dopaminergic neurotoxicity due to chronic PQ injections (Prasad et al., 2009; Qin et al., 2015). Our findings support the published data suggesting that PQ may not be as toxic to striatal neurons as initially assumed, despite modest but significant induction of CHOP and COX2 expression that may facilitate dopaminergic neural loss if given over a longer span of time or alternatively given in conjunction with other pesticides such as maneb. While TPPU did not significantly reduce the induction of pro-inflammatory COX2 mRNA, its effect on CHOP expression suggests that TPPU could potentially reduce PQ induced neuronal loss, because CHOP is a vital player in ER stress mediated neurodegeneration (Li et al., 2015b).

Furthermore, our study offers insight into the efficacy of EET regioisomers in mitigating TLR4 dependent glial activation, which underlies the neuroinflammatory response against many environmental neurotoxicants including PQ, organophosphate pesticides, dioxins, and ionizing radiation (Lucas and Maes, 2013; Yang et al., 2022). More specifically, we observed the effect of TPPU on enhancing the anti-inflammatory effect of all EET regioisomers that may be degraded by intracellular sEH activity, particularly of the 14,15-EET, which is also consistent with previous findings (Morisseau et al., 2010; Yu et al., 2000). Moreover, our data validate the anti-inflammatory effect of TPPU against TLR4-induced inflammation, hypothesized to underlie P-induced inflammation.

The *in vitro* efficacy of TPPU in this prophylactic study offers avenues to investigate the effects of sEH inhibitors against xenobiotic-induced neuroinflammation and toxicity. Increased efficacy of the natural EET chemical mediators' activity due to stabilization by the sEH inhibitor TPPU is consistent with previous findings on the presence of sEH enzyme expression and activity on mice and rat microglia and astrocytes (Atone et al., 2020). However, it should be noted that EETs may act differently *in vivo* compared to *in vitro*, due to the multifaceted effects of EETs including their anti-apoptotic and vasodilative effects, in addition to having different efficacy against toxins with different toxicodynamic profiles. Therefore, the differences in the effects of EETs regioisomers may vary on a case-by-case basis. While beyond the scope of this initial investigation, a more comprehensive study using multiple age groups and time points may be needed to have a more accurate view of the magnitude of inflammatory and ER stress responses due to PQ exposure. Older mice exhibit PQ-induced dopaminergic neurotoxicity more

robustly than younger mice (Thiruchelvam et al., 2003) and thus might be a more suitable model to assess the efficacy of sEH inhibition against PQ toxicity.

Neuroinflammation and induction of ER stress are thought to mediate toxicity of environmental neurotoxicants ranging from heavy metals and pesticides to industrial chemicals (Iqubal et al., 2020; Kraft and Harry, 2011). This study adds to the evidence that PQ may induce striatal inflammation and ER stress, though not as robustly as initially hypothesized. While PQ has long been associated with PD etiology, many of the behavioral symptoms observed in an MPTP model of PD including tremors, rigidity, or akinesia (Taylor et al., 2010) have not been observed in this study. There are many studies indicating that PQ could act synergistically with the pesticide maneb (Gupta et al., 2010; Thiruchelvam et al., 2000) or iron (Peng et al., 2007) among others to induce PD-like symptoms in mice. However, several studies have shown that there are nearly twice as many PD patients exposed to PQ alone compared to exposure to both PQ and maneb (Costello et al., 2009; Wang et al., 2011), suggesting that while maneb co-exposure could increase the risk of developing PD, effects and treatment options to sole exposure to PQ should continue to be investigated.

While the unique properties of PQ make environmental exposure routes low, PQ is one of the most acutely lethal pesticides used globally in many crops and thus occupational exposure can be high [3]. While PQ is often implicated as an environmental contributor to the PD etiology (Bastias-Candia et al., 2019; Dwyer et al., 2021), its chronic neurological impact is still unclear, especially in regard to cofactors such as age, gender, sex, genetic predispositions, as well as its interaction with other pesticides (Gupta et al.,

2010; Picillo et al., 2017). The chronic effects of this major pesticide on human and animal health remain elusive. Further research into the neurotoxic impact of chronic PQ exposure in various settings, along with confirmation of sEH inhibition and stabilization of endogenous EpFA is needed.

Acknowledgements and Conflicts of Interest:

Acknowledgments: This work was partially supported by the RIVER award (NIEHS/R35 ES030443), Superfund Research Program award (NIEHS/P42 ES004699), and the CounterACT award (NIH/US54 NS127758). In addition, we would like to acknowledge the laboratory of Dr. Heike Wulff for their continuous support and guidance. The content is solely the responsibility of the authors and does not necessarily represent the official views of the National Institutes of Health.

Conflict of interest statement: BD Hammock is a founder and KM Wagner is an employee of EicOsis L.L.C., a startup company with an sEH inhibitor in human clinical trials.

Table 1. Primer sequences for mouse and rat genes analyzed with RT-qPCR

Gene	Type	Sequence (5'-3')
Mouse primers for brain tissue		
ATF4	Forward	GACCTGGAAACCATGCCAGA
	Reverse	TGGCCAATTGGGTTCACTGT
BiP	Forward	ACTTGGGGACCACCTATTCCT
	Reverse	ATCGCCAATCAGACGCTCC
CHOP	Forward	CCCTGCCTTTCACCTTGG
	Reverse	CCGCTCGTTCTCCTGCTC
COX2	Forward	CAGACAACATAAACTGCGCCTT
	Reverse	GATACACCTCTCCACCAATGACC
GAPDH	Forward	CGTGTTCCTACCCCCAATGT
	Reverse	GTGTAGCCCAAGATGCCCTT
IL-1β	Forward	CCTTCCAGGATGAGGACATGA
	Reverse	TGAGTCACAGAGGATGGGCTC
sXBP1	Forward	GGTCTGCTGAGTCCGCAGCAGG
	Reverse	AGGCTTGGTGTATACATGG
TNF-α	Forward	GCCACCACGCTCTTCTGT
	Reverse	GGAGGCCATTTGGGAACT
Rat primers for cell culture		
CXCL1	Forward	ACTCAAGAATGGTCGCGAGG
	Reverse	ACGCCATCGGTGCAATCTAT
CXCL10	Forward	CGGTGAGCCAAAGAAGGTCTA
	Reverse	TGTCCATCGGTCTCAGCACT
GAPDH	Forward	CCAGGGCTGCCTTCTCTTGT
	Reverse	GTTTCCCGTTGATGACCAGC
GDNF	Forward	CACCAGATAAACAAGCGGCG
	Reverse	TCGTAGCCCAAACCCAAGTC
IL-1β	Forward	CTACCTATGTCTTGCCCGTGG
	Reverse	CACACTAGCAGGTCGTCATCA
IL-6	Forward	GGCTAAGGACCAAGACCATCC
	Reverse	GACCACAGTGAGGAATGTCCA
NOS2	Forward	TTTGACCAGAGGACCCAGAGA
	Reverse	CAGAGTGAGCTGGTAGGTTCC
COX2	Forward	ACGGTGAAACTCTAGACAGACA
	Reverse	AGGATACACCTCTCCACCGA

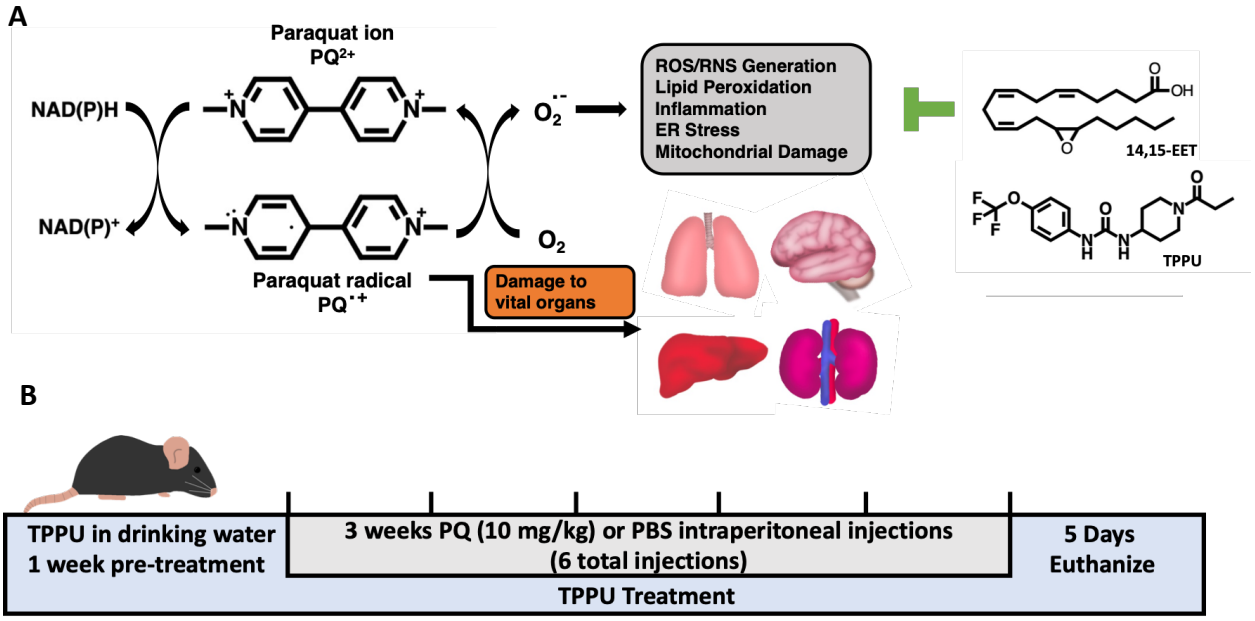

Figure 1. Schematic representations of the **A.** mechanism of PQ toxicity showing the structure of PQ and its radical form, as well as the 14,15-EET regioisomer and sEH inhibitor TPPU which stabilizes EpFA from hydrolysis by the sEH, and **B.** timeline of PQ injections in mice. PQ is thought to exert its toxic effects through redox cycling, whereby a PQ ion is converted into a PQ radical through a transfer of electrons from donors such as cytosolic NAD(P)H, which then generates oxygen radical leading to oxidative damage, lipid peroxidation, inflammation, ER stress, mitochondrial damage, and apoptosis. Acute exposure to PQ could result in kidney, liver, or respiratory failure, whereas long-term exposure to PQ may result in pulmonary fibrosis or damage to kidney and heart. Several studies have also shown that PQ distributes to and accumulates in the brain as well. Inhibitors of sEH enzyme acting to stabilize EpFA such as EETs are known to reduce inflammation, ER stress, pathological fibrosis, and apoptosis in many animal models. We therefore hypothesize that the administration of the sEH inhibitor TPPU will mitigate inflammation and ER stress in the brain of mice exposed to PQ.

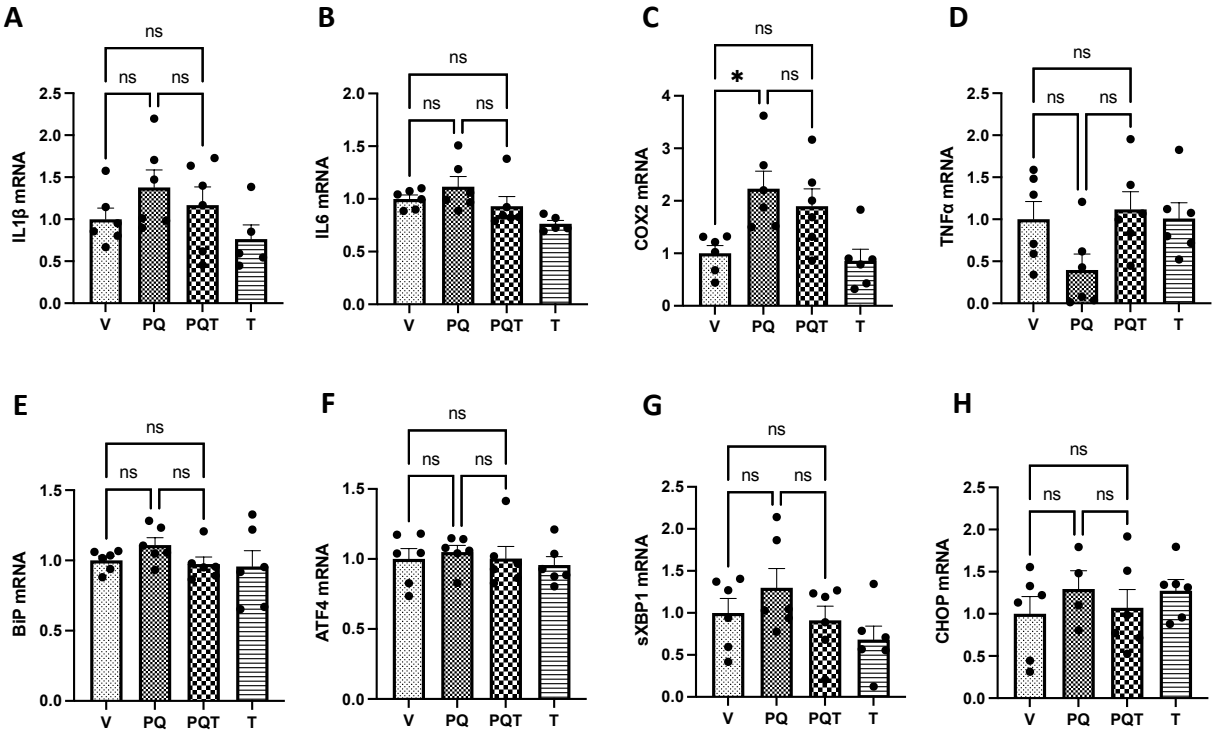

Figure 2. Effect of PQ and TPPU on striatal GAPDH normalized mRNA expressions of pro-inflammatory (**A-D**) and ER stress (**E-H**) markers. Chronic PQ treatment caused a non-significant increase of inflammatory genes **A.** IL-1β and **B.** IL-6, and a significant change in **C.** COX2 expression (p=0.0122). **D.** While there was some reduction of TNF-α in the PQ group (p=0.131) that was reversed by TPPU treatment (p=0.056), such effects were not statistically significant. However, the reduction of IL-1β, IL-6, and COX2 expressions by TPPU were not statistically significant. There was no detectable trend in changes in any of the ER stress gene expressions (**E-H**). Results are expressed as mean ± SEM. RT-qPCR, data represent 6 biological replicates. PCR results were normalized to respective GAPDH levels. Abbreviations: V = vehicle, PQ = paraquat, PQT = paraquat, TPPU, T = TPPU only control. *P < 0.05 and **P<0.01, as determined by one-way ANOVA or Kruskal-Wallis test followed by Dunnett's post-hoc test.

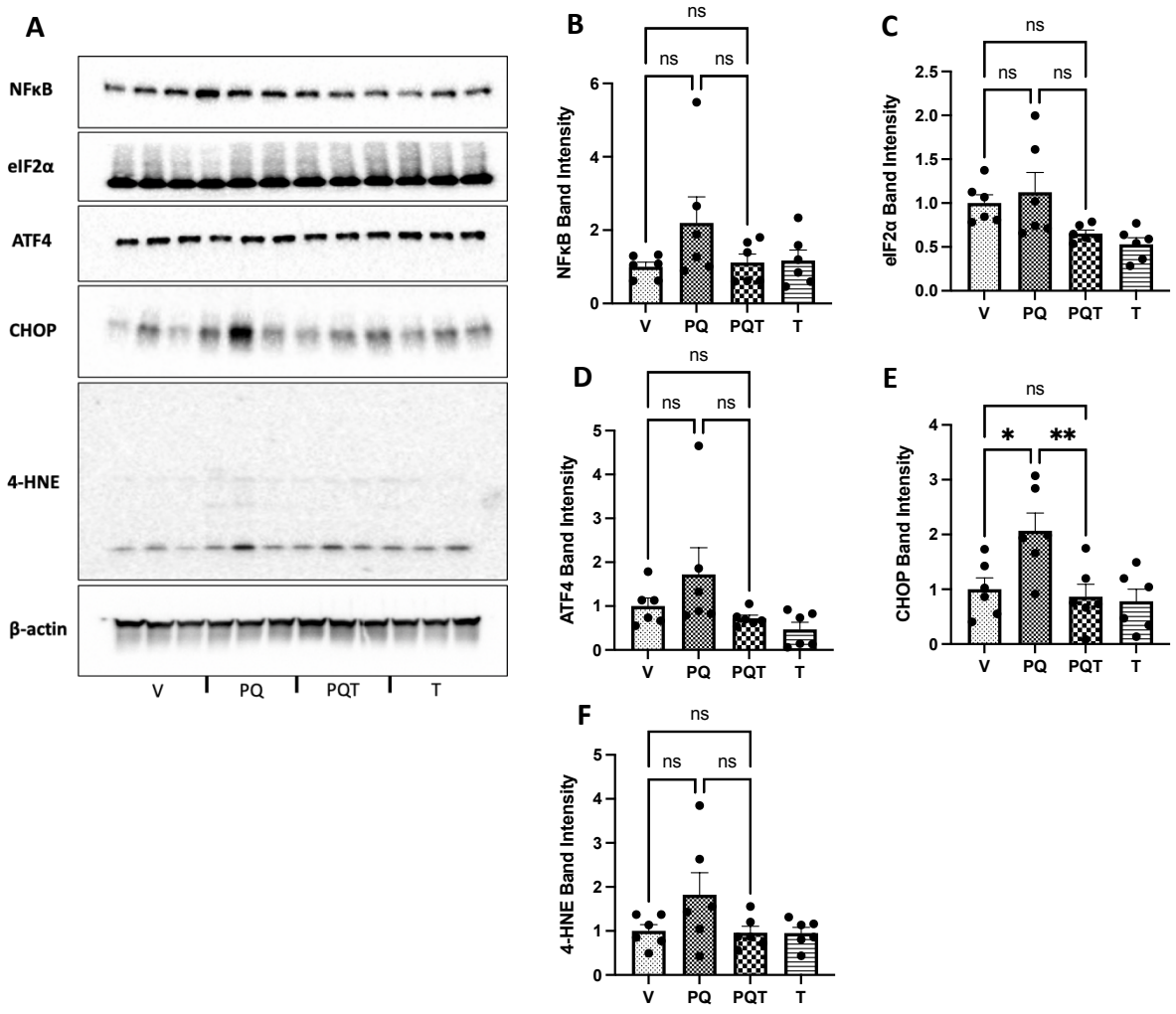

Figure 3. **A.** Western blot analysis of frozen striatum samples assessing protein levels of **B.** NF-κB, **C.** ATF4, **D.** eIF2α, **E.** CHOP, and **H.** 4-HNE. While PQ significantly increased CHOP protein expression (p=0.019), which was reduced by TPPU treatment (p=0.008), increases in other proteins due to PQ treatment were not statistically significant. Results are expressed as mean ± SEM, data represent 6 biological replicates. Western Blot results were normalized to β-actin. Abbreviations: V = vehicle, PQ = paraquat, PQT = paraquat and TPPU, T = TPPU only control. Results are expressed as mean ± SEM. *P < 0.05 and **P<0.01, as determined by one-way ANOVA or Kruskal-Wallis test followed by Dunnett's post-hoc test.

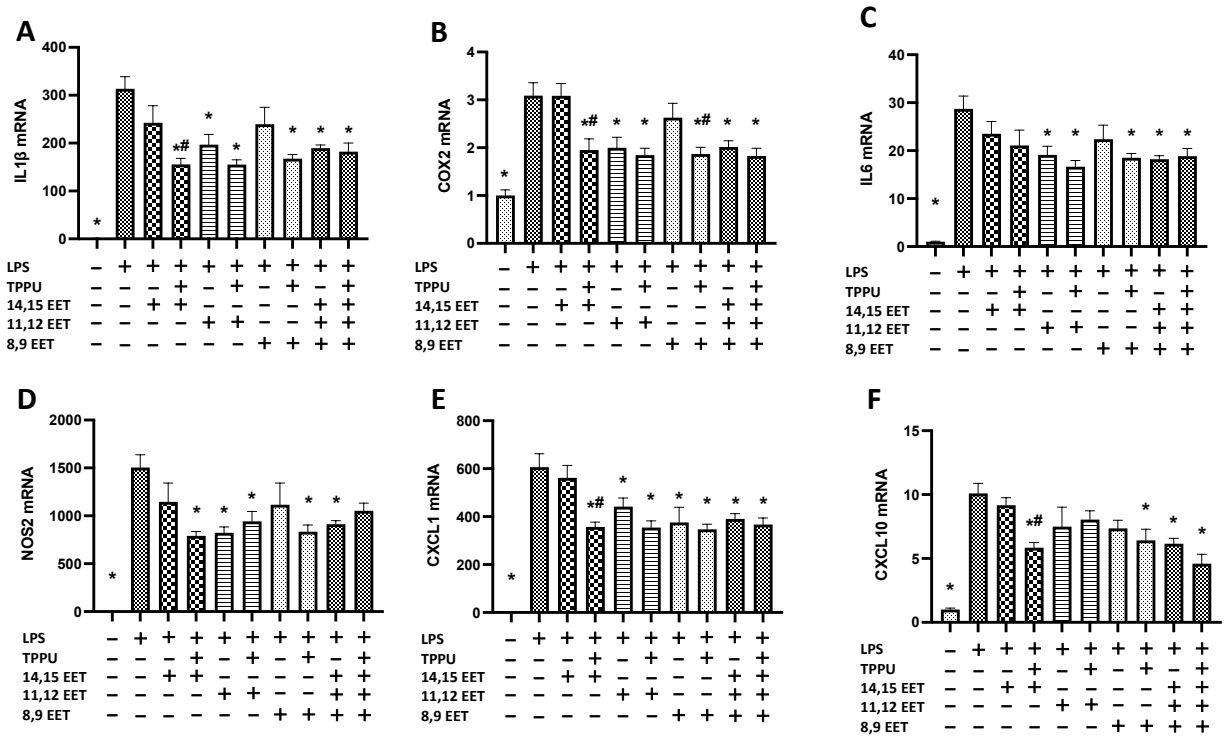

Figure 4. Primary rat glial cells (DIV 8-10) were pretreated with 1 μM of EET regioisomers in the absence or presence of TPPU (1 μM) and were then incubated with 300 ng/ml LPS in 100 μL DMEM for 24 hours. (**A-F**) LPS significantly increased inflammatory markers IL-1β, IL-6, COX2, NOS2, CXCL1, and CXCL10 mRNA expression (n=5 or 6 technical replicates, $p<0.001$), which were mitigated by EETs regioisomers, with a 1:1:1 ratio mixture of three EETs regioisomers, or EETs with TPPU cotreatment. While EETs regioisomers by themselves showed equivocal efficacy against LPS-induced inflammation, most EETs regioisomers mitigated LPS-induced inflammation when co-treated with TPPU ($p<0.05$). More specifically, TPPU treatment resulted in a significant reduction of IL-1β, COX2, CXCL1, and CXCL10 expressions when combined with 14,15-EET and COX2 expression when combined with 8,9-EET ($p<0.05$). Results are expressed as mean ± SEM. Statistical significance was determined by one-way ANOVA followed by Dunnett's post-hoc test (* $p<0.05$ compared to LPS; # $p<0.05$ compared to respective EET regioisomer without TPPU).

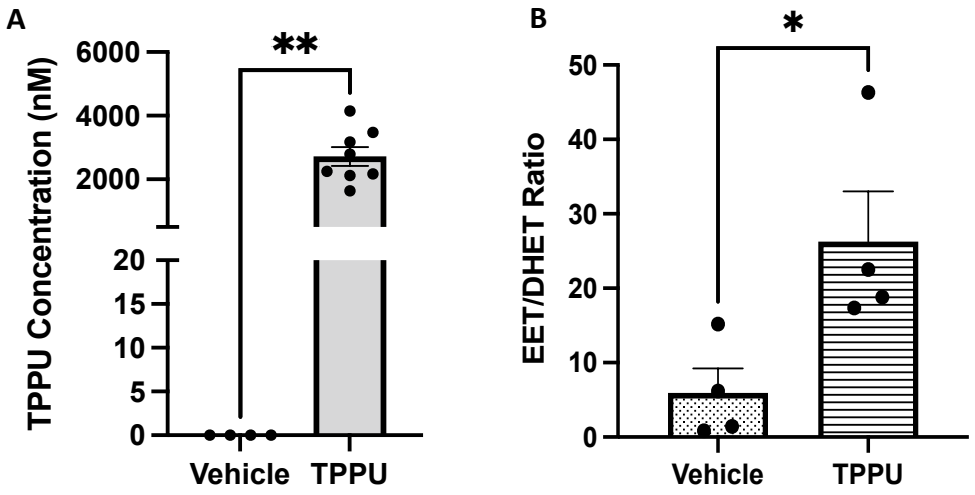

Figure S1. LC/MS analysis of murine blood and plasma. **A.** Peripheral TPPU concentration was assessed using whole blood collected from the tail vein from mice upon the completion of chronic TPPU treatment. Although there was some variability in the detected concentration, at least 1 μM of TPPU was detected in all mice tested (n=4 or 8, $p<0.001$), which is orders of magnitude above the IC_{50} of 6 nM (K_i of 600 pM), whereas no TPPU was detected in the control mice (n=4). **B.** Whole blood was collected via cardiac puncture and plasma was isolated and analyzed for changes in EET to DHET ratio. Chronic TPPU treatment has significantly increased the EET/DHET ratio (n=4, p=0.036). *P < 0.05 and **P<0.01, as determined by Two-tailed t-test. Bars represent ±SEM.

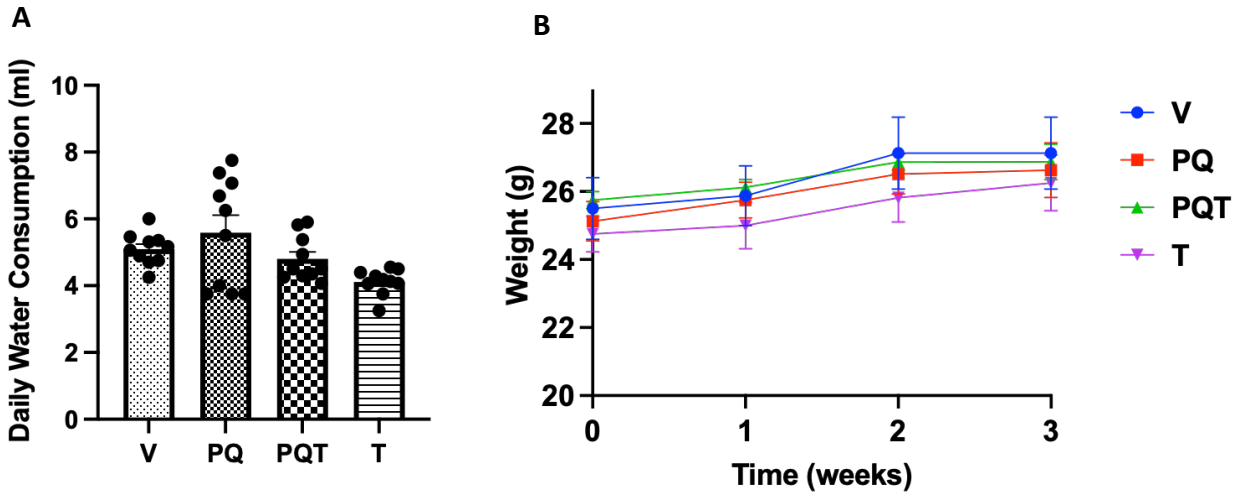

Figure S2. Measures of **A.** the estimated amount of water consumed per mouse per day, calculated from the total decrease in water volume by cage, and **B.** the mean weight of the mice in each treatment group (n=8). Mice in the TPPU group were slightly lighter than vehicle control mice (p=0.009) and drank less water than the vehicle control group (p=0.016), likely due to their lower initial weight. Abbreviations: V = vehicle, PQ = paraquat, PQT = paraquat and TPPU, T = TPPU only control. Results are expressed as mean ± SEM. Statistical significance was determined by Kruskal-Wallis test or repeated measures one-way ANOVA followed by Dunnett's post-hoc test.

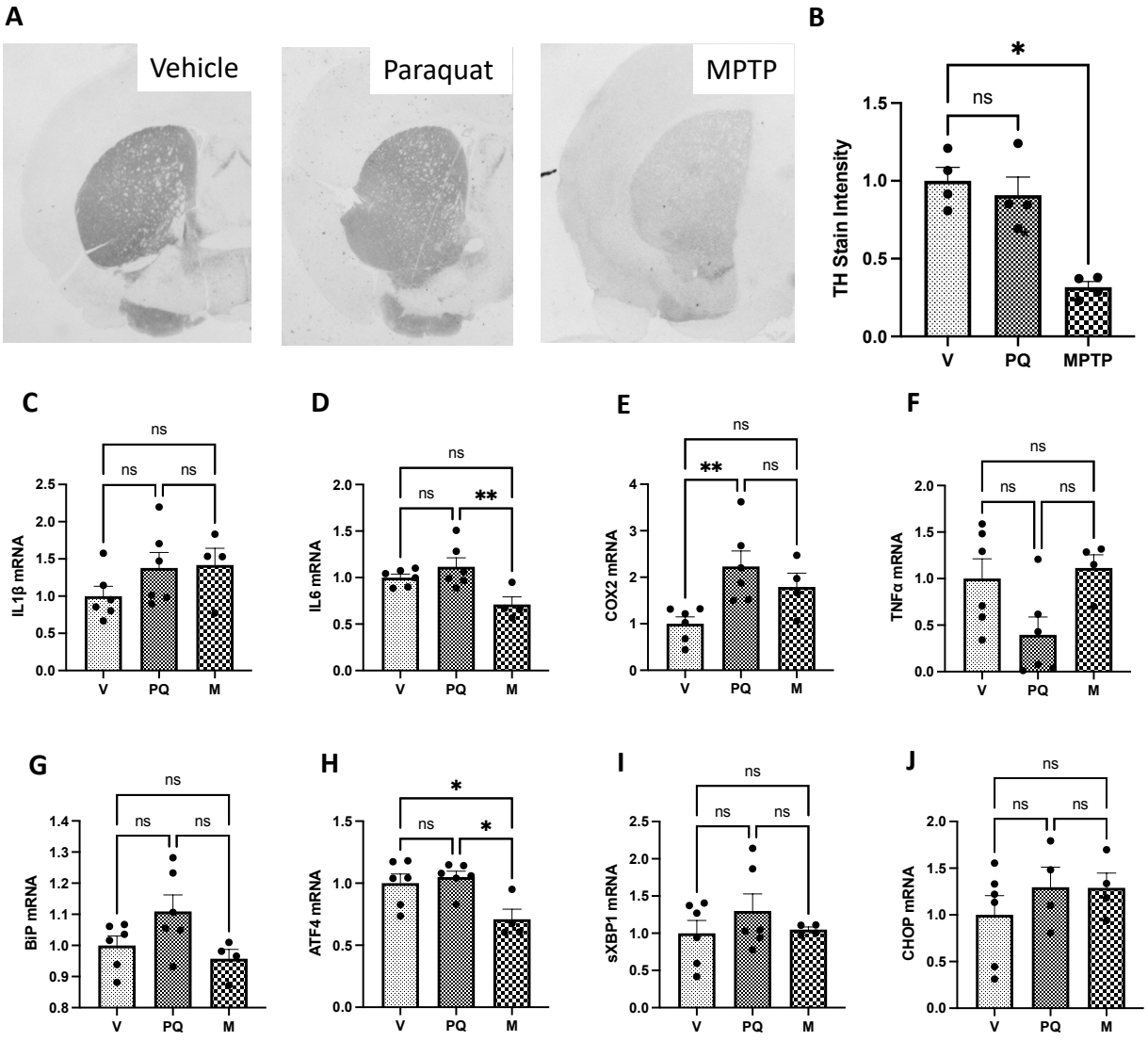

Figure S3. Immunohistochemical analysis of striatal expression of tyrosine hydroxylase and RT-qPCR of striatal mRNA. Mice were treated with MPTP (10 mg/kg/day, *i.p.*) in sterile PBS for five days and were euthanized five days post final injection to compare its effects to those of PQ treatment. (**A-B**) While MPTP resulted in a significant decrease of tyrosine hydroxylase indicative of dopaminergic neural loss (n=4, $p<0.001$), it did not significantly increase any inflammatory or ER stress markers. (**C-J**) MPTP resulted in a reduced GAPDH normalized mRNA expressions of IL-6 ($p=0.005$) and ATF4 ($p=0.014$) compared to PQ treatment, and reduced ATF4 ($p=0.039$) compared to vehicle control. Vehicle and PQ data are equal to those presented in Figure 3. MPTP treatment was conducted simultaneously with the PQ treatment. Abbreviations: V = vehicle, PQ = paraquat, M = MPTP. Results are expressed as mean ± SEM. *P < 0.05 as determined by one-way ANOVA or Kruskal-Wallis test followed by Dunnett's post-hoc test.

References

Atone, J., Wagner, K., Hashimoto, K., Hammock, B.D., 2020. Cytochrome P450 derived epoxidized fatty acids as a therapeutic tool against neuroinflammatory diseases. Prostaglandins Other Lipid Mediat 147, 106385.

Bastias-Candia, S., Zolezzi, J.M., Inestrosa, N.C., 2019. Revisiting the Paraquat-Induced Sporadic Parkinson's Disease-Like Model. Mol Neurobiol 56, 1044-1055.

Breckenridge, C.B., Sturgess, N.C., Butt, M., Wolf, J.C., Zadory, D., Beck, M., Mathews, J.M., Tisdel, M.O., Minnema, D., Travis, K.Z., Cook, A.R., Botham, P.A., Smith, L.L., 2013. Pharmacokinetic, neurochemical, stereological and neuropathological studies on the potential effects of paraquat in the substantia nigra pars compacta and striatum of male C57BL/6J mice. Neurotoxicology 37, 1-14.

Bromilow, R.H., 2004. Paraquat and sustainable agriculture. Pest Manag Sci 60, 340-349.

Campbell, J.L., Jr., Travis, K.Z., Clewell, H.J., 3rd, Stevens, A.J., Hinderliter, P.M., Andersen, M.E., Botham, P.A., Cook, A.R., Minnema, D.J., Wolf, D.C., 2021. Integration of paraquat pharmacokinetic data across species using PBPK modelling. Toxicol Appl Pharmacol 417, 115462.

Carroll, M.A., Balazy, M., Margiotta, P., Falck, J.R., McGiff, J.C., 1993. Renal vasodilator activity of 5,6-epoxyeicosatrienoic acid depends upon conversion by cyclooxygenase and release of prostaglandins. J Biol Chem 268, 12260-12266.

Costello, S., Cockburn, M., Bronstein, J., Zhang, X., Ritz, B., 2009. Parkinson's disease and residential exposure to maneb and paraquat from agricultural applications in the central valley of California. Am J Epidemiol 169, 919-926.

Dawson, A.H., Eddleston, M., Senarathna, L., Mohamed, F., Gawarammana, I., Bowe, S.J., Manuweera, G., Buckley, N.A., 2010. Acute human lethal toxicity of agricultural pesticides: a prospective cohort study. PLoS Med 7, e1000357.

Dinis-Oliveira, R.J., Remiao, F., Carmo, H., Duarte, J.A., Navarro, A.S., Bastos, M.L., Carvalho, F., 2006. Paraquat exposure as an etiological factor of Parkinson's disease. Neurotoxicology 27, 1110-1122.

Dwyer, Z., Rudyk, C., Farmer, K., Beauchamp, S., Shail, P., Derksen, A., Fortin, T., Ventura, K., Torres, C., Ayoub, K., Hayley, S., 2021. Characterizing the protracted neurobiological and neuroanatomical effects of paraquat in a murine model of Parkinson's disease. Neurobiol Aging 100, 11-21.

Ghosh, A., Comerota, M.M., Wan, D., Chen, F., Propson, N.E., Hwang, S.H., Hammock, B.D., Zheng, H., 2020. An epoxide hydrolase inhibitor reduces neuroinflammation in a mouse model of Alzheimer's disease. Sci Transl Med 12.

Gupta, S.P., Patel, S., Yadav, S., Singh, A.K., Singh, S., Singh, M.P., 2010. Involvement of nitric oxide in maneb- and paraquat-induced Parkinson's disease phenotype in mouse: is there any link with lipid peroxidation? Neurochem Res 35, 1206-1213.

Hung, T.H., Shyue, S.K., Wu, C.H., Chen, C.C., Lin, C.C., Chang, C.F., Chen, S.F., 2017. Deletion or inhibition of soluble epoxide hydrolase protects against brain damage and reduces microglia-mediated neuroinflammation in traumatic brain injury. Oncotarget 8, 103236-103260.

Iqubal, A., Ahmed, M., Ahmad, S., Sahoo, C.R., Iqubal, M.K., Haque, S.E., 2020. Environmental neurotoxic pollutants: review. Environ Sci Pollut Res Int 27, 41175-41198.

Jackson-Lewis, V., Blesa, J., Przedborski, S., 2012. Animal models of Parkinson's disease. Parkinsonism Relat Disord 18 Suppl 1, S183-185.
Jiang, H., McGiff, J.C., Quilley, J., Sacerdoti, D., Reddy, L.M., Falck, J.R., Zhang, F., Lerea, K.M., Wong, P.Y., 2004. Identification of 5,6-trans-epoxyeicosatrienoic acid in the phospholipids of red blood cells. J Biol Chem 279, 36412-36418.
Klintworth, H., Garden, G., Xia, Z., 2009. Rotenone and paraquat do not directly activate microglia or induce inflammatory cytokine release. Neurosci Lett 462, 1-5.
Kraft, A.D., Harry, G.J., 2011. Features of microglia and neuroinflammation relevant to environmental exposure and neurotoxicity. Int J Environ Res Public Health 8, 2980-3018.
Lakkappa, N., Krishnamurthy, P.T., M, D.P., Hammock, B.D., Hwang, S.H., 2019. Soluble epoxide hydrolase inhibitor, APAU, protects dopaminergic neurons against rotenone induced neurotoxicity: Implications for Parkinson's disease. Neurotoxicology 70, 135-145.
Lei, Y., Li, X., Yuan, F., Liu, L., Zhang, J., Yang, Y., Zhao, J., Han, Y., Ren, J., Fu, X., 2017. Toll-like receptor 4 ablation rescues against paraquat-triggered myocardial dysfunction: Role of ER stress and apoptosis. Environ Toxicol 32, 656-668.
Li, H.F., Zhao, S.X., Xing, B.P., Sun, M.L., 2015a. Ulinastatin suppresses endoplasmic reticulum stress and apoptosis in the hippocampus of rats with acute paraquat poisoning. Neural Regen Res 10, 467-472.
Li, Y., Guo, Y., Tang, J., Jiang, J., Chen, Z., 2015b. New insights into the roles of CHOP-induced apoptosis in ER stress. Acta Biochim Biophys Sin (Shanghai) 47, 146-147.
Lucas, K., Maes, M., 2013. Role of the Toll Like receptor (TLR) radical cycle in chronic inflammation: possible treatments targeting the TLR4 pathway. Mol Neurobiol 48, 190-204.
Mandel, J.S., Adami, H.O., Cole, P., 2012. Paraquat and Parkinson's disease: an overview of the epidemiology and a review of two recent studies. Regul Toxicol Pharmacol 62, 385-392.
McGeer, P.L., McGeer, E.G., 2004. Inflammation and neurodegeneration in Parkinson's disease. Parkinsonism Relat Disord 10 Suppl 1, S3-7.
Morisseau, C., Inceoglu, B., Schmelzer, K., Tsai, H.J., Jinks, S.L., Hegedus, C.M., Hammock, B.D., 2010. Naturally occurring monoepoxides of eicosapentaenoic acid and docosahexaenoic acid are bioactive antihyperalgesic lipids. J Lipid Res 51, 3481-3490.
Peng, J., Peng, L., Stevenson, F.F., Doctrow, S.R., Andersen, J.K., 2007. Iron and paraquat as synergistic environmental risk factors in sporadic Parkinson's disease accelerate age-related neurodegeneration. J Neurosci 27, 6914-6922.
Picillo, M., Nicoletti, A., Fetoni, V., Garavaglia, B., Barone, P., Pellecchia, M.T., 2017. The relevance of gender in Parkinson's disease: a review. J Neurol 264, 1583-1607.
Prasad, K., Tarasewicz, E., Mathew, J., Strickland, P.A., Buckley, B., Richardson, J.R., Richfield, E.K., 2009. Toxicokinetics and toxicodynamics of paraquat accumulation in mouse brain. Exp Neurol 215, 358-367.
Qin, X., Wu, Q., Lin, L., Sun, A., Liu, S., Li, X., Cao, X., Gao, T., Luo, P., Zhu, X., 2015. Soluble epoxide hydrolase deficiency or inhibition attenuates MPTP-induced parkinsonism. Molecular neurobiology 52, 187-195.
Ramakers, C., Ruijter, J.M., Deprez, R.H., Moorman, A.F., 2003. Assumption-free analysis of quantitative real-time polymerase chain reaction (PCR) data. Neurosci Lett 339, 62-66.

Ren, Q., Ma, M., Yang, J., Nonaka, R., Yamaguchi, A., Ishikawa, K.-i., Kobayashi, K., Murayama, S., Hwang, S.H., Saiki, S., 2018. Soluble epoxide hydrolase plays a key role in the pathogenesis of Parkinson's disease. Proceedings of the National Academy of Sciences 115, E5815-E5823.
Rose, T.E., Morisseau, C., Liu, J.Y., Inceoglu, B., Jones, P.D., Sanborn, J.R., Hammock, B.D., 2010. 1-Aryl-3-(1-acylpiperidin-4-yl)urea Inhibitors of Human and Murine Soluble Epoxide Hydrolase: Structure-Activity Relationships, Pharmacokinetics, and Reduction of Inflammatory Pain. Journal of Medicinal Chemistry 53, 7067–7075.
See, W.Z.C., Naidu, R., Tang, K.S., 2022. Cellular and Molecular Events Leading to Paraquat-Induced Apoptosis: Mechanistic Insights into Parkinson's Disease Pathophysiology. Mol Neurobiol 59, 3353-3369.
Seok, S.J., Gil, H.W., Jeong, D.S., Yang, J.O., Lee, E.Y., Hong, S.Y., 2009. Paraquat intoxication in subjects who attempt suicide: why they chose paraquat. Korean J Intern Med 24, 247-251.
Simpkins, A.N., Rudic, R.D., Schreihofer, D.A., Roy, S., Manhiani, M., Tsai, H.J., Hammock, B.D., Imig, J.D., 2009. Soluble epoxide inhibition is protective against cerebral ischemia via vascular and neural protection. Am J Pathol 174, 2086-2095.
Singh, N., Vik, A., Lybrand, D.B., Morisseau, C., Hammock, B.D., 2021. New Alkoxy-Analogues of Epoxyeicosatrienoic Acids Attenuate Cisplatin Nephrotoxicity In Vitro via Reduction of Mitochondrial Dysfunction, Oxidative Stress, Mitogen-Activated Protein Kinase Signaling, and Caspase Activation. Chem Res Toxicol 34, 2579-2591.
Smeyne, R.J., Breckenridge, C.B., Beck, M., Jiao, Y., Butt, M.T., Wolf, J.C., Zadory, D., Minnema, D.J., Sturgess, N.C., Travis, K.Z., Cook, A.R., Smith, L.L., Botham, P.A., 2016. Assessment of the Effects of MPTP and Paraquat on Dopaminergic Neurons and Microglia in the Substantia Nigra Pars Compacta of C57BL/6 Mice. PLoS One 11, e0164094.
Srikrishna, V., Riviere, J.E., Monteiro-Riviere, N.A., 1992. Cutaneous toxicity and absorption of paraquat in porcine skin. Toxicol Appl Pharmacol 115, 89-97.
Tangamornsuksan, W., Lohitnavy, O., Sruamsiri, R., Chaiyakunapruk, N., Norman Scholfield, C., Reisfeld, B., Lohitnavy, M., 2019. Paraquat exposure and Parkinson's disease: A systematic review and meta-analysis. Arch Environ Occup Health 74, 225-238.
Taylor, T.N., Greene, J.G., Miller, G.W., 2010. Behavioral phenotyping of mouse models of Parkinson's disease. Behav Brain Res 211, 1-10.
Thiruchelvam, M., Brockel, B.J., Richfield, E.K., Baggs, R.B., Cory-Slechta, D.A., 2000. Potentiated and preferential effects of combined paraquat and maneb on nigrostriatal dopamine systems: environmental risk factors for Parkinson's disease? Brain Res 873, 225-234.
Thiruchelvam, M., McCormack, A., Richfield, E.K., Baggs, R.B., Tank, A.W., Di Monte, D.A., Cory-Slechta, D.A., 2003. Age-related irreversible progressive nigrostriatal dopaminergic neurotoxicity in the paraquat and maneb model of the Parkinson's disease phenotype. Eur J Neurosci 18, 589-600.
Tu, R., Armstrong, J., Lee, K.S.S., Hammock, B.D., Sapirstein, A., Koehler, R.C., 2018. Soluble epoxide hydrolase inhibition decreases reperfusion injury after focal cerebral ischemia. Sci Rep 8, 5279.
USGS, 2021. Estimated Annual Agricultural Pesticide Use, Pesticide National Synthesis Project,

https://water.usgs.gov/nawqa/pnsp/usage/maps/show_map.php?year=2018&map=PARAQUAT&hilo=H (accessed 31 August 2022)
Wagner, K.M., McReynolds, C.B., Schmidt, W.K., Hammock, B.D., 2017. Soluble epoxide hydrolase as a therapeutic target for pain, inflammatory and neurodegenerative diseases. Pharmacol Ther 180, 62-76.
Wan, D., Yang, J., McReynolds, C.B., Barnych, B., Wagner, K.M., Morisseau, C., Hwang, S.H., Sun, J., Blocher, R., Hammock, B.D., 2019. In vitro and in vivo Metabolism of a Potent Inhibitor of Soluble Epoxide Hydrolase, 1-(1-Propionylpiperidin-4-yl)-3-(4-(trifluoromethoxy)phenyl)urea. Front Pharmacol 10, 464.
Wang, A., Costello, S., Cockburn, M., Zhang, X., Bronstein, J., Ritz, B., 2011. Parkinson's disease risk from ambient exposure to pesticides. Eur J Epidemiol 26, 547-555.
Wu, X.F., Block, M.L., Zhang, W., Qin, L., Wilson, B., Zhang, W.Q., Veronesi, B., Hong, J.S., 2005. The role of microglia in paraquat-induced dopaminergic neurotoxicity. Antioxid Redox Signal 7, 654-661.
Yang, H.M., Wang, Y.L., Liu, C.Y., Zhou, Y.T., Zhang, X.F., 2022. A time-course study of microglial activation and dopaminergic neuron loss in the substantia nigra of mice with paraquat-induced Parkinson's disease. Food Chem Toxicol 164, 113018.
Yang, J., Schmelzer, K., Georgi, K., Hammock, B.D., 2009. Quantitative profiling method for oxylipin metabolome by liquid chromatography electrospray ionization tandem mass spectrometry. Anal Chem 81, 8085-8093.
Yang, Z., Shao, Y., Zhao, Y., Li, Q., Li, R., Xiao, H., Zhang, F., Zhang, Y., Chang, X., Zhang, Y., Zhou, Z., 2020. Endoplasmic reticulum stress-related neuroinflammation and neural stem cells decrease in mice exposure to paraquat. Sci Rep 10, 17757.
Yoshida, H., 2007. ER stress and diseases. FEBS J 274, 630-658.
Yu, Z., Xu, F., Huse, L.M., Morisseau, C., Draper, A.J., Newman, J.W., Parker, C., Graham, L., Engler, M.M., Hammock, B.D., Zeldin, D.C., Kroetz, D.L., 2000. Soluble epoxide hydrolase regulates hydrolysis of vasoactive epoxyeicosatrienoic acids. Circ Res 87, 992-998.